Adaptive Active Control of Machine-Tool Vibration in a Lathe

I. Claesson[(1)] and L. Håkansson[(2)]

[(1)]Department of Signal Processing, University of Karlskrona/Ronneby, 372 25 Ronneby, Sweden

[(2)]Department of Production and Materials Engineering, Lund University, Box 118, 221 00 Lund, Sweden

In turning operations the relative dynamic motion between the cutting tool and workpiece, or vibration, is a frequent problem. This affects the results of the machining, and in particular, the surface finish. Tool life is also influenced by vibration. Noise in the working environment frequently occurs as a result of dynamic motion between the cutting tool and the workpiece. With proper machine design, i.e. improved stiffness of the machine structure, the problem of relative dynamic motion between the cutting tool and workpiece may be partially solved. However, by use of active control of the machine-tool vibration, a further reduction of the dynamic motion between the cutting tool and workpiece can be achieved. It was found that adaptive feedback control of the tool vibration in the cutting speed direction, based on the fil-tered-x LMS-algorithm, enables a reduction in vibration, by up to 40 dB at 1.5 kHz, and by approximately 40 dB at 3 kHz. It was also observed that the introduction of leakage in the filtered-x LMS-algorithm improved the stability properties of the feedback control system. A significant improvement in the workpiece surface finish was observed and a substantial reduction in the noise level was obtained with adaptive control.

1. INTRODUCTION

In turning operations the tool and tool holder shank are subjected to dynamic excitation due to the deformation of the work material during the cutting operation. The stochastic chip formation process usually induces vibrations in the machine-tool system. Energy from the chip formation process excites the mechanical modes of the machine-tool system. Modes of the workpiece may also influence tool vibration. The relative dynamic motion between the cutting tool and workpiece will affect the result of the machining, in particular the surface finish. Furthermore, the tool life is correlated with the amount of vibration and the acoustic noise introduced. The noise is sometimes almost unbearable for the operator.

It is well known that vibration problems are closely related to the dynamic stiffness of the structure of the machinery and workpiece material. The vibration problem may be solved in part by proper machine design leading to a stiffer machine structure. In order to achieve further improvements the dynamic stiffness of the tool holder shank can be increased more selectively. One solution to these problems is active control of the tool vibrations.

Generally, machine-tool systems are classified as narrow-band systems[1] and as a consequence tool shank vibrations can usually be described as a superposition of narrow-band random processes at each modal frequency. These when added together form a more wide-band random process.[1] The tool vibrations in a turning operation mainly comprise vibrations in two directions: the cutting speed direction and the feed direction.[1,2] Usually, the vibrations in the cutting speed direction and the feed direction are linearly independent, except at some of the eigenfrequencies.[1] Consequently, the control problem involves the introduction of two secondary sources, driven in such a way that the anti-vibrations generated by means of these sources interfere destructively with the tool vibration.[3] However, in external longitudinal turning, most of the vibration energy is usually induced in the cutting speed direction.[1,2] It is thus likely that the control of tool vibration in the cutting speed direction is an adequate solution to the vibration problem.[2,4] A complication in the turning operation is that the original excitation of the tool vibration in the chip formation process cannot be observed directly and thus cannot be used as a feedforward control signal.

The statistical properties of the tool vibration imply a controller which utilizes the statistical correlation of the vibrations.[5] A classical statistical criterion is the mean square error criterion.[6] However, a controller based on this criterion cannot generally solve the control problem, since such a controller is only "optimum" in a stationary environment.[7] The statistical properties of the tool vibrations may vary during the machining process. Changes in cutting data and material properties influence the statistical properties of tool vibrations.[1,2] Variation within the allowed cutting data interval may also influence the structural response of the tool holder.[2] In the case of constant cutting data, adaptive feedback control of machine-tool vibration based on the well known filtered-x LMS-algorithm seems very promising.[2] However, variations within the excitation and the structural response of the tool holder influence the stability of the adaptive feedback control system. The stability of the feedback control system is affected by the ability of the filtered-x LMS-algorithm to control the adaptive FIR filter, the time varying controller response, without violating the closed-loop stability requirements, i.e. the Nyquist stability criterion.[8] A solution to the control problem is to control the adaptive FIR filter with the leaky version of the filtered-x LMS-algorithm.[4]

This paper discusses single-channel feedback control of tool vibration in the cutting speed direction. The single channel control system is illustrated in Fig. 1.

The tool holder in this application has integrated actuators, i.e. secondary sources, which have been developed at DPME (Department of Production and Materials Engineering, Institute of Technology, Lund University).[9] The construction of the tool holder is shown in Fig. 2.

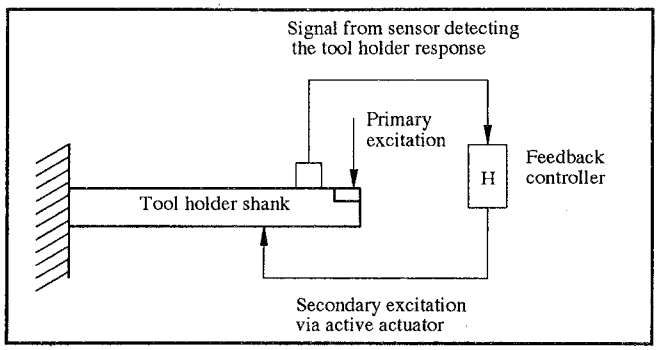

Figure 1. A machine-tool feedback control system.[2]

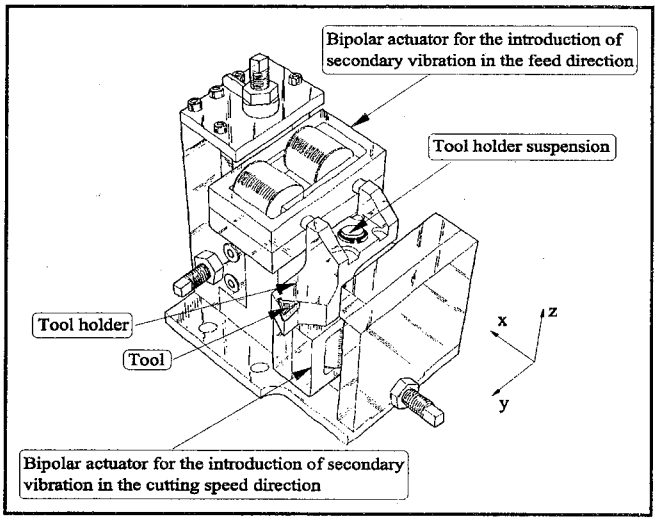

Figure 2. Tool holder with integrated actuators for the control of tool vibration in the metal cutting process.[9]

2. MATERIALS AND METHODS

2.1. Experimental Set-Up

The cutting experiments were carried out on a Köping lathe with 6 kW spindle power using a tool holder construction with integrated actuators.[9] An accelerometer mounted on the cutting tool made it possible to measure the vibrations in the cutting speed direction. The tool holder construction is based on two bipolar actuators. The bipolar design is motivated by a desire to achieve linear behaviour. This is composed of two actuators that work with a 180° phase difference. The actuators are based on high magnetostrictive material. In order to operate the bipolar actuator, a large current amplifier (5 kW) was used. A digital signal processor controller was used and the measurements were carried out on a two-channel signal analyzer. Furthermore, a two channel low-pass filter was used to adjust the input level to the A/D converter and the output level from the D/A converter.

2.1.1. Work Material — Cutting Data — Tool Geometry

The workpiece material SS 2541-03, chromium molybdenum nickel steel,[1] was used in the experiments. This work material excites the machine-tool-system with a narrow bandwidth in the cutting operation. After a preliminary set of trials, a suitable combination of cutting data and tool geometry was selected (see Table 1). The combination was selected to cause significant tool vibrations. These resulted in an observable deterioration of the workpiece surface, and severe acoustic noise. The diameter of the workpiece is intentionally large, over 100 mm, in order to render workpiece vibrations negligible.

Table 1. Cutting data and tool geometry.

Geometry	DNMG 150604-PF 4015
Cutting speed v (m/min)	80
Depth of cut a (mm)	0.9
Feed s (mm/rev)	0.25

2.2. Tool Shank Vibration

The tool shank vibrations obtained are random in nature. These are usually characterized by more than one vibration mode, except in the case of the lowest feed rate and cutting speed.[1] If a linear model can be assumed, the time-domain dynamic response of the tool holder is determined by the mode superposition principle.[1,10] Each modal displacement is determined by a convolution integral, a mechanical filtering-denoted Duhamel's integral[10] — where the input is the dynamic generalized load. The modal response of the filter is determined by the modal damping ratio, the generalized modal mass, the generalized modal load, as well as the eigenfrequencies for the damped and undamped system.

Machine-tool systems are usually classified as narrow-band systems.[1] Hence, most structural systems have reasonably low damping; and if the damping ratio ξ is less than 0.1, they are classified as narrow-band systems.[10] Consequently tool shank vibrations can generally be described as a superposition of narrow-band random processes at each modal frequency, which when added together form a more wide-band random process.[1,10] The modal behaviour of the tool shank vibrations is obvious from Fig. 3, which shows the estimated spectral densities of dynamic responses typical of a tool holder shank. The spectral densities are measured in the cutting speed direction during a continuous cutting operation in SS 0727-02. A constant feed rate, $s = 0.3$ mm/rev, was used for different cutting speeds between 50 m/min and 400 m/min in intervals of 25 m/min.

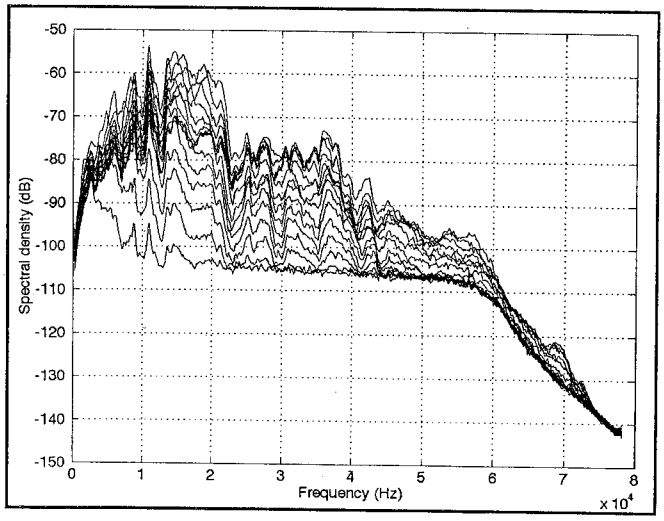

Figure 3. The estimated spectral densities of the dynamic response of the tool holder shank in the cutting speed direction during a continuous cutting operation. Workpiece material SS 0727-02, feed rate $s = 0.3$ mm/rev, cut depth $a = 3$ mm, cutting speed $v = 50$ m/min to 400 m/min, tool DNMG-QM 150612, grade 4025.[1]

2.3. Adaptive Control of Tool Vibration

The excitation of the tool vibrations originating from the material deformation process cannot be directly observed. Consequently, the controller for the reduction of machine-tool vibration is based on a feedback approach. The response of the tool holder can be measured with a sensor mounted on the machine-tool. By introducing anti-vibrations with a secondary source actuator the response of the tool holder can be modified.[2] The actuator is steered by a controller fed with the accelerometer signal which senses the vibrations of the tool holder (see Fig. 1).

Adaptive digital FIR filters based on the method of steepest descent are popular in various application areas, e.g. active control of sound,[5,7] active control of vibration[2,11] and in other applications, such as electrical noise cancelling, system identification, adaptive beam-forming, etc.[12,13] This is due to the simplicity of the implementation and the unimodal error surface in the feedforward application. A feedforward active controller can easily be controlled to converge towards a feasible solution.[12] Adaptive FIR filters are usually used in feedforward control[5,7] but can also be used in feedback control,[3,14] although there is no guarantee that the error surface will be unimodal under such conditions.[15] Similar problems can also be observed in feedforward control systems, when the control problem is ill-conditioned. A method to improve such systems is to add a leakage factor to the adaptation algorithm.[16] This will also have the effect of limiting the energy in the impulse response of the adaptive filter, which is likely to be advantageous in the case of feedback control. Furthermore, the leakage factor will also prevent accumulative build-up of bias in the coefficients of the adaptive filter.[17]

2.3.1. The Adaptive Algorithm

The objective of the control scheme is to minimize the mean square error. The use of the error signal as the input signal to the adaptive FIR filter controlling the plant, will cause the adaptive FIR filter to act as a feedback controller. This will complicate the relation between the mean square error and the filter coefficients, i.e. the mean square error will not be a quadratic function of the filter coefficients. In fact the mean square error function may be multimodal in the filter coeffi- cients.[18]

A block diagram of the adaptive feedback control system based on an adaptive FIR filter is shown in Fig. 4. The box with the unit delay operator q^{-1} at the input to the controller is inherent to the involvement of an adaptive digital filter in a feedback control system. The search for a minimum on the mean square error surface can be performed by an algorithm based on the steepest-descent method.

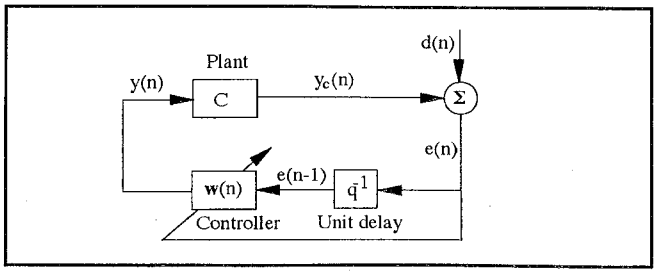

Figure 4. Block diagram of an active feedback control system using an adaptive FIR filter.

A stochastic gradient algorithm for control application is given by

$$y(n) = \mathbf{w}^T(n)\mathbf{x}(n), \tag{1}$$

$$e(n) = d(n) - c(n) * y(n), \tag{2}$$

$$\mathbf{w}(n+1) = \mathbf{w}(n) - \tfrac{1}{2}\mu\nabla e^2(n), \tag{3}$$

where $*$ is the convolution operator, $c(n)$ is the impulse response of the forward path, $\nabla e^2(n)$ is the gradient vector of the squared error signal with respect to $\mathbf{w}(n)$, and $\mathbf{w}(n)$ is the $M\times 1$ coefficient vector of an adaptive FIR filter. Furthermore, the reference signal $x(n)$ supplied to the adaptive algorithm is given by

$$x(n) = e(n-1). \tag{4}$$

The gradient of the squared error can be expressed as

$$\nabla e^2(n) = 2[\nabla e(n)]\, e(n). \tag{5}$$

In order to derive an expression for the gradient vector the derivative of the error signal with respect to each coefficient is taken. This is given by

$$\frac{\partial e(n)}{\partial w_m(n)} = -c(n) * \frac{\partial y(n)}{\partial w_m(n)}. \tag{6}$$

Here, it is assumed that the desired signal $d(n)$ is independent of the filter coefficients. The partial derivative on the right hand side can be expanded as

$$\frac{\partial e(n)}{\partial w_m(n)} = -c(n) * \left(e(n-m-1) + \sum_{j=0}^{M-1} w_j(n) \frac{\partial e(n-j-1)}{\partial w_m(n)} \right). \tag{7}$$

Neglecting the derivatives of past estimation errors with respect to the filter coefficients, a simplified derivative of the error signal with respect to each coefficient is obtained;

$$\frac{\partial e(n)}{\partial w_m(n)} = -c(n) * e(n-m-1). \tag{8}$$

Thus, the simplified gradient of the squared error can be written as

$$\nabla e^2(n) = -c(n) * \begin{bmatrix} e(n-1) \\ e(n-2) \\ \vdots \\ e(n-M) \end{bmatrix} e(n). \tag{9}$$

Further, by assuming that the transfer function for the secondary path can be modelled with an Ith-order FIR filter, with coefficients c_i^*, $i \in \{0,\ldots,I-1\}$, the simplified gradient of the squared error can be expressed as

$$\nabla e^2(n) = -\mathbf{x}_{C^*}(n) e(n), \tag{10}$$

where $\mathbf{x}_{C^*}(n)$ is given by

$$\mathbf{x}_{C^*}(n) = \begin{bmatrix} \sum_{i=0}^{I-1} c_i^* e(n-i-1) \\ \sum_{i=0}^{I-1} c_i^* e(n-i-2) \\ \vdots \\ \sum_{i=0}^{I-1} c_i^* e(n-i-M) \end{bmatrix}. \tag{11}$$

Inserting the simplified gradient of the squared error, Eq. (10), in Eq. (3) the following gradient algorithm is obtained:

$$y(n) = \mathbf{w}^T(n)\mathbf{x}(n), \tag{12}$$

$$e(n) = d(n) - y_C(n),\ y_C(n) = c(n) * y(n), \tag{13}$$

$$\mathbf{w}(n+1) = \mathbf{w}(n) + \mu \mathbf{x}_{C^*}(n)e(n). \tag{14}$$

This is the conventional filtered-x LMS-algorithm.[7] However, observe the feedback relation from $x(n) = e(n-1)$.

The estimation error is given by the recursive difference equation:

$$e(n) = -c(n) * \sum_{m=0}^{M-1} w_m(n)e(n-m-1) + d(n). \tag{15}$$

This expression can be rewritten in a more convenient form using delay-operator notation as follows:

$$e(n) = -C(q)W(n,q)q^{-1}e(n) + d(n), \tag{16}$$

which can be expressed as the filtering operation:

$$e(n) = \frac{1}{1 + C(q)W(n,q)q^{-1}}\, d(n). \tag{17}$$

From this expression it is obvious that the poles of the filter, i.e. the poles of the transfer function between the desired signal $d(n)$ and the estimation error $e(n)$, are affected by the controller response. The stability of the feedback control system thus depends on the ability of the filtered-x LMS-algorithm to control the adaptive FIR filter, the time varying controller response, without violating the closed loop stability requirements, i.e. the Nyquist stability criterion.[8] In feedback control, limiting the energy in the control signal to the plant yields a more robust behaviour. By introducing leakage in the filtered-x LMS-algorithm the "memory" of the adaptive algorithm is reduced thereby reducing the energy in the response of the adaptive FIR filter and also the energy in the control signal to the plant.

The leaky version of the filtered-x LMS-algorithm is obtained through a modification of the algorithm for the coefficient vector adaptation of the filtered-x LMS-algorithm with a leakage factor γ. As a result, the algorithm for the coefficient vector adaptation of the leaky version of the filtered-x LMS-algorithm is given by:[12]

$$\mathbf{w}(n+1) = \gamma \mathbf{w}(n) + \mu \mathbf{x}_{C^*}(n)e(n). \tag{18}$$

The leakage factor γ is a real positive parameter which satisfies the condition:

$$0 < \gamma < 1. \tag{19}$$

In order to select a step length μ to enable the filtered-x LMS algorithm to converge, the following inequality is commonly used:[19]

$$0 < \mu < \frac{2}{E[x^2_{C^*}(n)](M+\delta)}, \tag{20}$$

where δ is the overall delay in the forward path, M is the length of the adaptive FIR filter and $E[x^2_{C^*}(n)]$ is the mean square value of the filtered reference signal to the algorithm.

2.3.2. The Adaptive Control System

The controller used in the experiments described here was of the feedback type based on the well-known filtered-x LMS-algorithm.[2,14] A block diagram of the feedback control system with the filtered-x LMS algorithm is shown in Fig. 5, where C represents the dynamic secondary system (forward path) under control, i.e. the electro-mechanical response. The estimate of this path is denoted by C^*.

The secondary path was estimated in an initial phase and was carried out by a second adaptive FIR filter steered by the LMS algorithm as in Fig. 6. In the estimation, a broadband normally-distributed training signal was used.

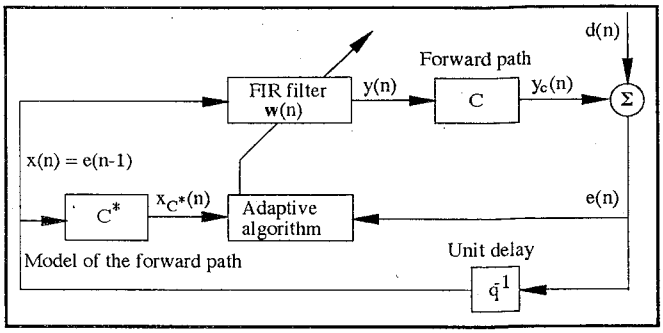

Figure 5. Equivalent block diagram of the feedback control situation with the filtered-x LMS algorithm.[2]

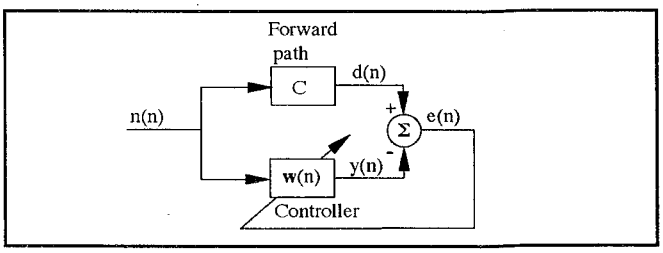

Figure 6. Block diagram of off-line forward path estimation.

The fixed FIR filter estimate of the forward path was subsequently used to prefilter the input signal to the algorithm for the adaptation of the coefficient vector in the filtered-x LMS algorithm.

In order to tune the filtered-x LMS algorithm, the upper limit for the step length μ_{max} was calculated according to Eq. (20). Both the mean-square value of the filtered reference signal and the overall delay in the forward path were estimated. Hence, the estimation of the mean-square value of the filtered reference signal was based on a vibration signal obtained without control. In Fig. 7 the Bode plot of the estimated frequency response for the forward path is given and in Fig. 8 the corresponding estimate of the coherence spectrum is shown.

The spectrum parameters used in the estimation of the frequency response for the forward path and the coherence spectrum are given in Table 2.

Using the phase function for the frequency response of the forward path, an estimate of the delay in the forward path was calculated, as shown in Fig. 9.

In the calculation of the upper limit of the step length, the overall delay was assumed to be $\delta = 10$ *samples*. This gave an upper limit for the step length of $\mu_{max} \approx 0.3$. To increase the probability of stable action of the filtered-x LMS algorithm in the experiments, the step length μ was initially set to $\mu = 0.05$.

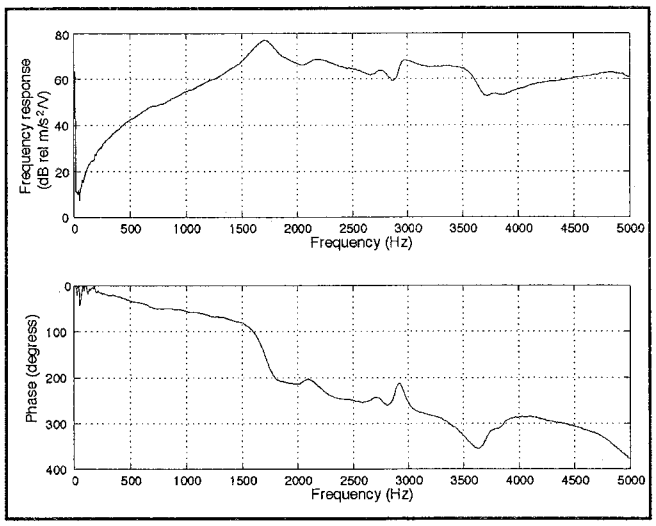

Figure 7. The estimated frequency response for the forward path.

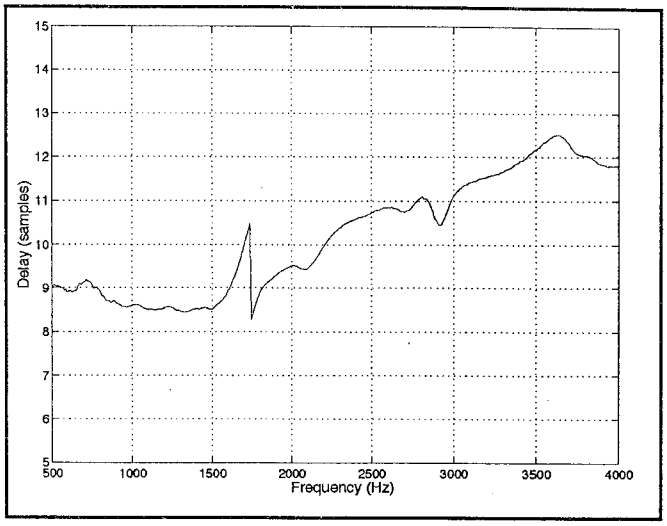

Figure 9. The estimated delay for the forward path.

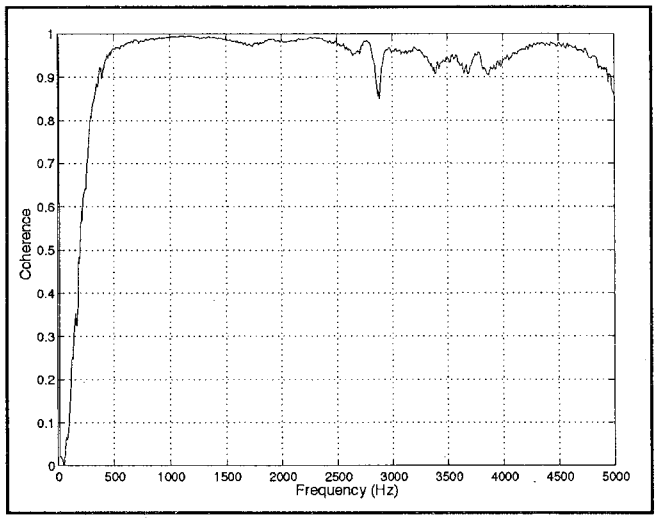

Figure 8. The estimated coherence spectrum between input and output signals for the forward path.

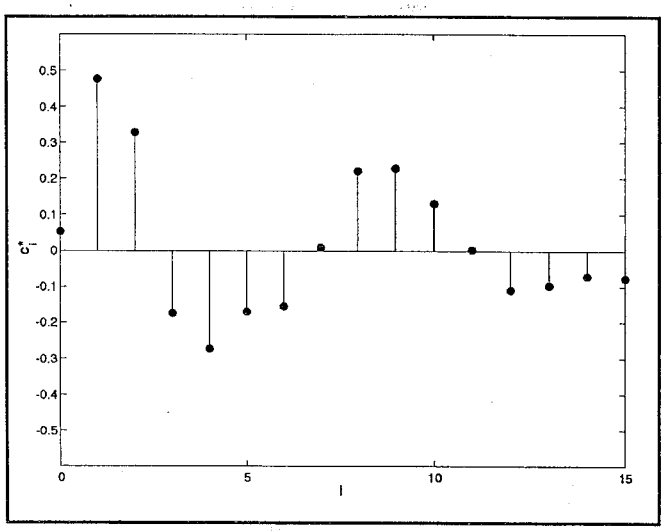

Figure 10. The coefficients of the 16-tap FIR filter estimate of the secondary path.

Table 2. Power spectral density estimation parameters used in the estimation of the frequency response for the forward path and the corresponding coherence spectrum.

Parameter	Value
Data segment length, L	2048
Number of periodograms, K	100
Digital window $w(\tau)$	Hanning
Sampling rate	16384 Hz

For the control of tool vibration a 20-tap adaptive FIR filter was used together with a 16-tap FIR filter estimate of the secondary path.[2] These filter lengths were at the limit of the processing capacity of the signal processor used. A typical secondary path estimate is shown in Fig. 10.

A 15 kHz sampling rate was chosen for the digital filter. In order to minimize delay in the loop, no anti-aliasing or reconstruction filters were used. Obviously, this necessitates extra care to be taken to avoid aliasing.

3. RESULTS

The tool shank vibrations considered in this paper originate from the cutting speed direction of the tool holder shank in the tool holder construction. To facilitate the results presented in the paper the dynamic responses of the tool shank in the tool holder construction is denoted with *tool vibration*.

To illustrate the effect of feedback control of tool vibration in the cutting speed direction, the spectral densities of the tool vibrations with and without feedback control are given. The spectral densities were estimated with an HP 35665A dynamic signal analyzer using Welch's method.[20] The parameters used for the power spectral density estimation are shown in Table 3.

Figure 11 shows a typical result obtained with adaptive feedback control of tool-vibration. This control performs a broad-band attenuation of the tool-vibration and manages to reduce the vibration level by up to approximately 40 dB simultaneously at 1.5 kHz and 3 kHz.

Figure 12 shows the vibration spectrum obtained using four different settings of the leakage factor in the adaptive al-

gorithm used in the 20-tap FIR filter feedback controller. To illustrate the influence of the leakage factor on the spectral properties of the tool vibration, the spectral densities are also given in a waterfall diagram (see Fig. 13).

Table 3. Power spectral density estimation parameters.

Parameter	Value
Data segment length, L	1024
Number of periodograms, K	50
Digital window $w(\tau)$	Hanning
Sampling rate	16384 Hz

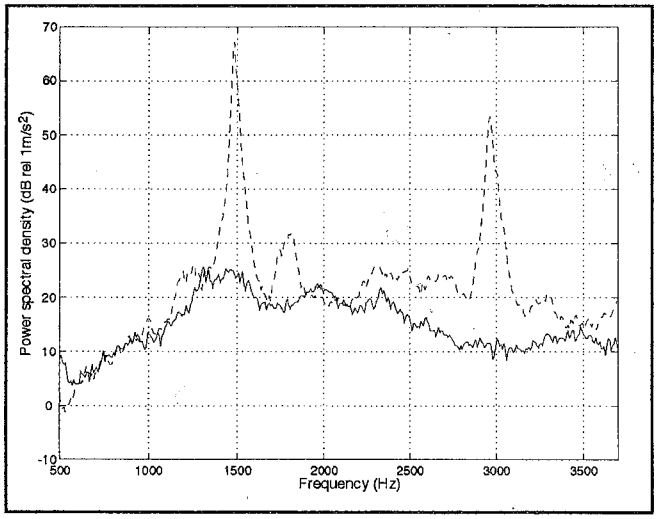

Figure 11. The power spectral density of tool vibration with 20-tap FIR filter feedback control (solid) and without (dashed). Step length $\mu = 0.05$, cutting speed $v = 80$ m/min, cut depth $a = 0.9$ mm, feed rate $s = 0.25$ mm/rev, tool DNMG 150604-PF, grade 4015.

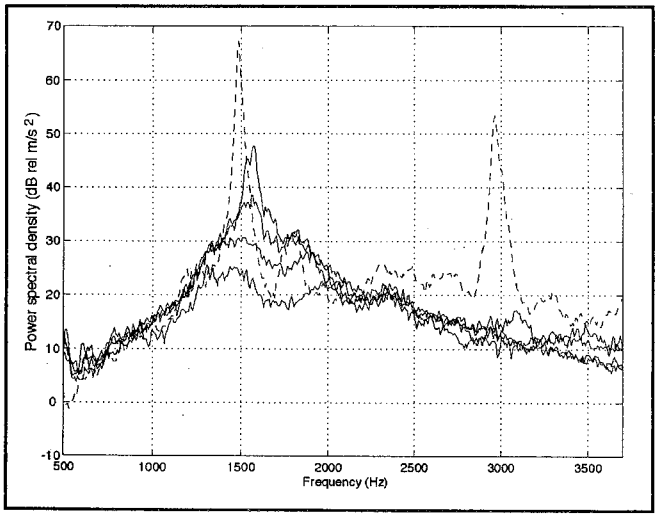

Figure 12. The power spectral densities of tool vibrations with 20-tap FIR filter feedback control and four different leakage factors (solid), and spectral density without feedback control (dashed). Leakage factors $\gamma = 1, 0.9999, 0.999, 0.99$, step length $\mu = 0.05$, cutting speed $v = 80$ m/min, cut depth $a = 0.9$ mm, feed rate $s = 0.25$ mm/rev, tool DNMG 150604-PF, grade 4015.

Furthermore, the influence of the leakage factor on the impulse response of the 20-tap adaptive FIR is shown in Fig. 14. In Fig. 15 the influence of leakage on the relative magnitude of the frequency response of the 20-tap adaptive FIR is illustrated. The corresponding relative magnitude of the frequency response of the 20-tap adaptive FIR in Fig. 14 is shown in Fig. 15 for the different settings of the leakage factors.

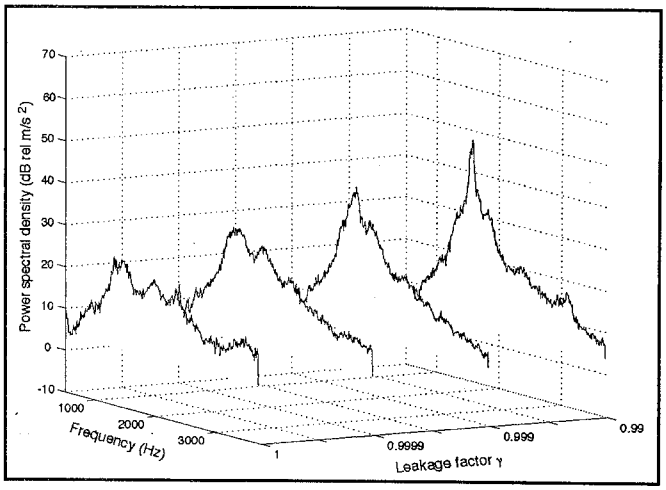

Figure 13. The Power spectral densities of tool vibrations with 20-tap FIR filter feedback control, and four different leakage factors. Leakage factors $\gamma = 1, 0.9999, 0.999, 0.99$, step length $\mu = 0.05$, cutting speed $v = 80$ m/min, cut depth $a = 0.9$ mm, feed rate $s = 0.25$ mm/rev, tool DNMG 150604-PF, grade 4015.

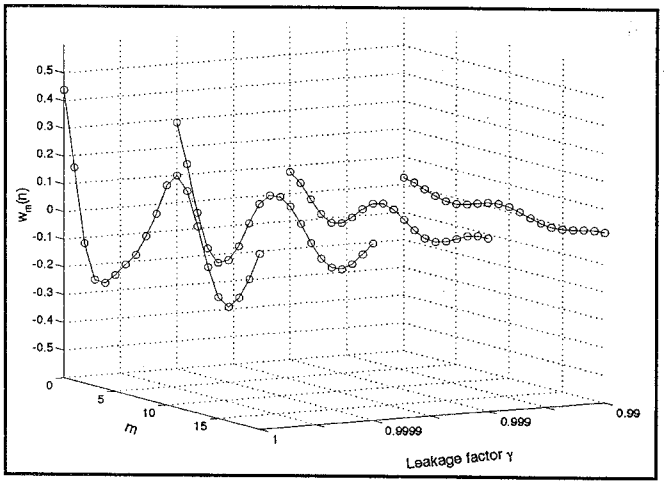

Figure 14. The coefficients of the 20-tap adaptive FIR filter for four different leakage factors. Leakage factors $\gamma = 1, 0.9999, 0.999, 0.99$, step length $\mu = 0.05$, cutting speed $v = 80$ m/min, cut depth $a = 0.9$ mm, feed rate $s = 0.25$ mm/rev, tool DNMG 150604-PF, grade 4015.

The stability of the feedback control system is affected by the ability of the filtered-x LMS-algorithm to control the adaptive FIR filter, the time-varying controller response, without violating the closed loop stability requirements, i.e. Nyquist stability criterion.[8] If the closed loop system is to be stable, the polar plot of the open loop frequency response for the feedback control system $C(f)W(f)$ must not enclose the $(-1, 0)$ on the Nyquist diagram. The larger the smallest distance between the polar plot and the $(-1, 0)$ point is, the more robust is the feedback control system with respect to variation in the controller response and forward path response.

To illustrate the influence of leakage on the stability of the feedback control system, the significant part of the Nyquist plot, i.e. the part of the Nyquist plot closest to the

point $(-1, 0)$, is given for estimates of the open loop frequency response with and without leakage in the filtered-x LMS algorithm. Figure 16 shows the Nyquist plot for the case of no leakage; and Figure 17 shows the Nyquist plot for the case of leakage in the filtered-x LMS algorithm. The spectrum parameters used in the estimation of the open loop frequency response are given in Table 4.

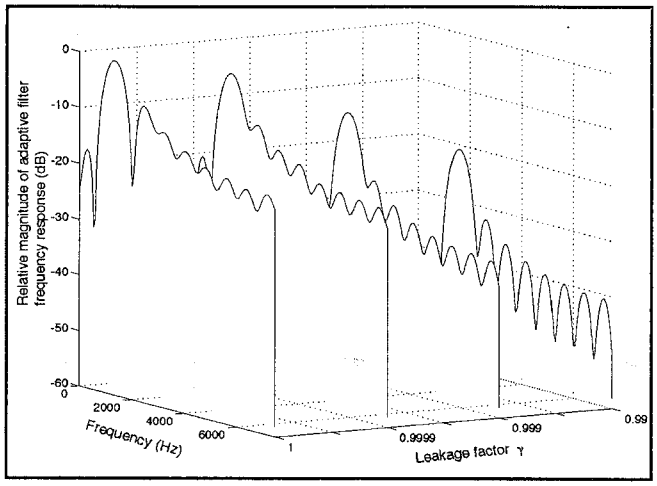

Figure 15. The relative magnitude of the frequency response of the 20-tap adaptive FIR filter for four different leakage factors. Leakage factors $\gamma = 1, 0.9999, 0.999, 0.99$, step length $\mu = 0.05$, cutting speed $v = 80$ m/min, cut depth $a = 0.9$ mm, feed rate $s = 0.25$ mm/rev, tool DNMG 150604-PF, grade 4015.

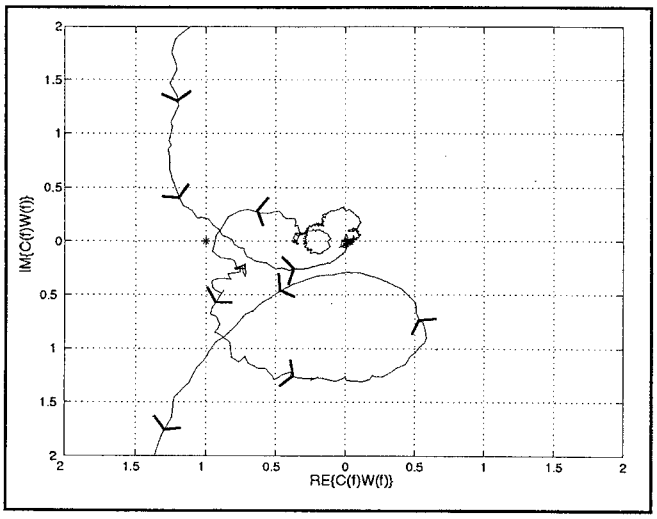

Figure 16. Nyquist diagram for the feedback control system without leakage, step length $\mu = 0.05$.

Table 4. Spectral density estimation parameters used for the estimation of open loop frequency response.

Parameter	Value
Data segment length, L	2048
Number of periodograms, K	200
Digital window $w(\tau)$	Hanning
Sampling rate	16384 Hz

In the experiments, it was observed that the adaptive feedback control led to a significant improvement in the workpiece surface finish, and a simultaneous reduction in the acoustic noise induced by tool vibration. Figure 18 shows a photo of the workpiece used in the experiments.

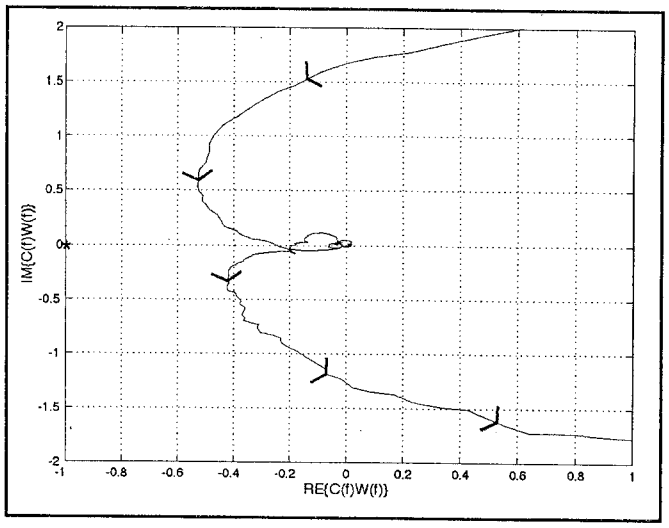

Figure 17. Nyquist diagram for the feedback control system with leakage, $\gamma = 0.999$, step length $\mu = 0.05$.

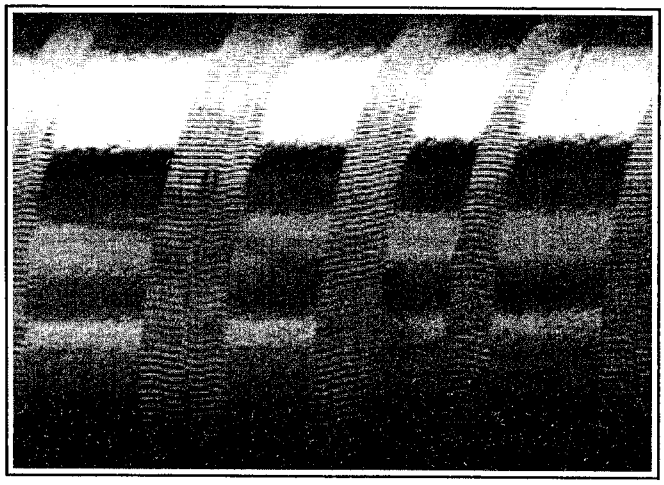

Figure 18. The workpiece surface with, and without, adaptive feedback control.

4. CONCLUSIONS AND FUTURE RESEARCH

It is clear that tool vibrations that occur in a lathe during metal cutting can be controlled using an active control system. The tool holder shank vibrations are fed into an actuator via a digital controller. Further, the well-known filtered-x LMS-algorithm, traditionally used as a feedforward controller, seems to have great potential with respect to feedback control of tool vibrations in the turning operation. The adaptive feedback control performs a broad-band attenuation of the tool-vibration, and is able to reduce the vibration level by up to approximately 40 dB simultaneously at 1.5 kHz and 3 kHz (see Fig. 11). It was found that the initial step length, $\mu = 0.05$, was a good choice and allows stable control while maintaining good attenuation of the tool vibration. Furthermore, in the experiments it was observed that the upper limit for the step length, to allow stable control, was approxi-

mately given by $\mu_{max} = 0.1$. However, when cutting data were varied the stability of the adaptive feedback control system was influenced. In order to improve the robustness of the feedback control with respect to variation in cutting data, leakage was introduced in the filtered-x LMS-algorithm.

As expected, the introduction of leakage reduced the performance of the adaptive control (see Figs. 12 and 13). However, it seems that the attenuation of the peak at 3 kHz is unaffected by the introduction of leakage. Thus, if the tool vibration is taken into consideration, the motion of the tool tip is limited by the workpiece in the direction of feed and in the reverse direction of cutting speed.[1] This is likely to introduce nonlinearities in the tool vibration.[1] A probable explanation as to why the introduction of leakage does not affect the attenuation of the peak at 3 kHz might be that the active control linearizes the tool vibration and thereby causes the reduction of the peak at 3 kHz. The introduction of a leakage factor or a "forgetting factor" in the recursive coefficient adjustment algorithm will induce bias in the coefficient vector (see Fig. 14), and thereby cause a somewhat reduced attenuation of the tool-vibration.

On the other hand, with the leaky version of the filtered-x LMS-algorithm a substantial improvement was observed in the robustness of the control system with respect to variations in cutting data. The system was provoked numerous times with varying cutting data but it remained stable. A probable explanation for the improved robustness of the control system obtained with the leaky version of the filtered-x LMS-algorithm is illustrated in Fig. 15. This implies that the leakage factor has the ability to reduce the magnitude of the frequency response of the adaptive FIR filter, i.e. it causes the loop gain of the control system to be reduced and thereby increases the distance between the polar plot of the open loop frequency response and the point $(-1,0)$. This can be observed by comparing the Nyquist diagram for the open loop response obtained without leakage shown in Fig. 16 and the Nyquist diagram for the open loop response obtained with leakage in Fig. 17.

From manufacturing and engineering points of view, the significant improvement in the workpiece surface as illustrated in Fig. 18, achieved with the adaptive feedback control of the tool vibration, is of great significance. The reduction in the noise level introduced by the tool vibrations is also an important feature. It is also interesting to note that the adaptive technique does not affect the cutting data; it may indeed even allow an increase in the material removal rate. Further, it is well known that there exists a correlation between tool vibration and tool life. It is thus likely that the adaptive feedback control of the tool vibration increases tool life.

Future work will include the investigation of Internal Modal Control based on the filtered-x LMS algorithm in the application. There is also an urgent need for the production of a theoretical foundation for the behaviour of the filtered-x LMS algorithm in this application.

ACKNOWLEDGMENTS

This project was sponsored by the Volvo Research Foundation and the Volvo Educational Foundation, and the National Swedish Board for Technical Development (NUTEK).

REFERENCES

1. Sturesson, P-O., Håkansson, L., and Claesson I. Identification of the Statistical Properties of the Cutting Tool Vibration in a Continuous Turning Operation - Correlation to Structural Properties, *Journal of Mechanical Systems and Signal Processing, Academic Press,* **11**(3), (1997).
2. Håkansson, L., Claesson, I., and Sturesson P-O. Adaptive Feedback Control of Machine-Tool Vibration based on The Filtered-x LMS Algorithm, *International Journal of Low Frequency Noise, Vibration and Active Control, to be published,* (1997).
3. Håkansson, L., Sturesson, P-O., and Claesson I. Active Control of Machine-Tool Vibration, *Proc. 6th International Conference on Manufacturing Engineering,* (1995).
4. Claesson, I., Håkansson, L. Active Control of Machine-Tool Vibration in a Lathe, *Proc. Fifth International Congress on Sound and Vibration,* Vol. 1, 501-510, (1997).
5. Elliott, S.J., Nelson, P.A. Active Noise Control, *IEEE signal processing magazine,* 12-35, October (1993).
6. Papoulis, A. *Probability, Random Variables, and Stochastic Processes,* McGraw-Hill, second edition, (1984).
7. Nelson, P.A., Elliott, S.J. *Active Control of Sound,* Academic Press, Inc., (1992).
8. Åström, K.J., Wittenmark, B. *Computer Controlled Systems, Theory and Design,* Prentice Hall, (1984).
9. Andersson, P. A tool holder construction with integrated actuators. Master's thesis report 9054, Department of Production and Materials Engineering, Institute of Technology, Lund University, (1990) (In Swedish).
10. Clough, R.W., Penzien J. *Dynamics of Structures,* McGraw-Hill, second edition, (1975).
11. Fuller, C.R., Elliott, S.J., and Nelson P.A. *Active Control of Vibration,* Academic Press, Inc., (1996).
12. Widrow, B., Stearns, S.D. *Adaptive Signal Processing,* Prentice-Hall, (1985).
13. Claesson, I., Nordholm, S., Bengtsson, B., and Eriksson, P. A Multi-DSP implementation of a Broadband Adaptive Beamformer for use in a Hands-free Mobile Radio Telephone, *IEEE Trans. on Vehicular Technology,* February (1991).
14. Stothers, I.M., Saunders, T.J., McDonald, A.M., and Elliott S.J. Adaptive Feedback Control of Sun Roof Flow Oscillations. *Proceedings of the Institute of Acoustics,* **15**, 383-393, (1993).
15. Billoud, G., Galland, M.A., Huu, C.H., and Candel S. Adaptive Active Control of Instabilities, *Proc. Recent Advances in Active Control of Sound and Vibration,* 95-107, (1991).
16. Elliott, S.J., Boucher, C.C., and Nelson, P.A. The Behavior of a Multiple Channel Active Control System, *IEEE Transactions on signal processing,* **40**(5), 1041-1052, (1992).
17. Cioffi, J.M. Limited-Precision Effects in Adaptive Filtering, *IEEE Transactions on circuits and systems,* CAS-34 (7), 821-833, (1987).
18. Elliott, S.J. Active Control Using Feedback, Technical Report 732, Institute of Sound & Vibration Research, University, January, (1994).
19. Kuo, S.M., Morgan, D.R. *Active Noise Control Systems,* Telecommunications and Signal Processing. Wiley, (1996).
20. Welch, P.D. The Use of Fast Fourier Transform for the Estimation of Power Spectra: A Method Based on Time Averaging Over Short, Modified Periodograms, *IEEE Transactions on Audio and Electroacoustics,* 70-73, June (1967).